



Numerical and experimental research on shafts with elliptical sections formed by cross wedge rolling

Junling Li¹ · Weicheng Chu¹ · Pengni Feng¹ · Baoyu Wang¹ · Ping Chen¹ · Shuang Fang²

Received: 9 October 2022 / Accepted: 22 May 2023 / Published online: 10 June 2023
© The Author(s), under exclusive licence to Springer-Verlag London Ltd., part of Springer Nature 2023

Abstract

Blades are important parts of aero-engines, and their manufacturing technology directly affects the preparation level and development speed of aero-engines. In view of the many problems existing in the current blade preforming process, this paper proposes a potential way to prepare blade preforms by using cross wedge rolling (CWR). Furthermore, considering the shape characteristics of the blade, a blade preform with an elliptical section formed by CWR was thoroughly investigated. The roll's profile curve is of significant importance to forming quality, and its equation was deduced based on the plane meshing principle between the roll and the rolling piece and verified by finite element (FE) analysis and CWR experiments on a homemade platform. Meanwhile, the accuracy of the established FE model was quantitatively tested and used to study the forming limit expressed by eccentricity e , and the forming limit was approximately 0.8 (i.e., $e \leq 0.8$). Based on this, a blade preform for an aero-engine compressor was designed with two elliptical sections, and it was well formed by the FE model, which verified the feasibility; these research results can also be extended and applied to the preform of other nonrotating parts and other materials.

Keywords Shaft with elliptical section · Cross wedge rolling · Blade preform · Titanium alloy · Forming limit

1 Introduction

Blades are one of the most important parts of aero-engines, and their manufacturing technology directly affects the preparation level and development speed of aero-engines. At present, the preform of a blade is mainly prepared by extrusion, upsetting, free forging and other processes and finally formed by die forging [1, 2]. However, the existing preforming processes have problems such as complicated procedures, high cost, poor organization uniformity and stability [3, 4]. Therefore, it is important to explore new methods for preforming blades with high performance, a short process and precise controllability.

Cross wedge rolling (CWR) is a near-net-shape process with high efficiency and material utilization that has been

widely used to produce shaft parts for vehicles, high-speed rails and other equipment [5–7]. Currently, a sufficient number of studies have been conducted to ensure the stable rolling of billets and the forming accuracy and performance of shafts formed by CWR. Li et al. discussed the optimization of CWR tool design based on an experimental investigation of the morphology of internal defects of circular section solid shafts formed by CWR [8]. Pater et al. explored the formability of circular section solid and hollow shafts with different configurations of CWR processes on the basis of theoretical and experimental studies [9, 10]. Ji et al. manufactured a circular section hollow valve preform with good forming quality via a variable stretching angle CWR die [11, 12]. Shen et al. revealed the formation mechanism of the inner hole spiral groove of circular section hollow shafts formed by CWR and summarized the applicable range of process parameters for ensuring the forming accuracy of the inner hole [13, 14]. This research demonstrated that various circular section shafts with high forming quality can be manufactured by selecting the appropriate CWR process parameters. Based on these factors, several researchers have successfully developed a combined process of CWR and isothermal forging to manufacture aero-engine turbine

✉ Junling Li
junlingli@ustb.edu.cn

¹ School of Mechanical Engineering, University of Science and Technology Beijing, No.30 Xueyuan Road, Haidian District, Beijing 100083, China

² Beijing Institute of Aeronautical Materials, Beijing 100095, China

blades of different materials [15–17]. First, a preform with a circular section of the turbine blade was formed by the CWR process, and then the final product was forged with the preform. The formability, microstructure, and mechanical properties of the rolling pieces in two processes were investigated by forming experiments and finite element (FE) simulations, and the results demonstrated that the turbine blades manufactured by the CWR and isothermal forging processes fully met the current technical requirements. However, for a complex-shaped titanium alloy blade with a damper platform and tenon, subsequent isothermal forging would be more advantageous to ensure that the billet fully fills the die forging cavity if a preform with a cross-sectional shape close to that of the blade could be produced, such as a shaft with an elliptical section, and the material utilization would be improved. Therefore, a turbine blade preform with an elliptical section formed by CWR is innovatively proposed in this paper.

Thus far, shaft parts with noncircular sections formed by CWR have been extensively studied. Liang et al. analyzed the geometric relationship between the CWR dies and the meshing moving edge of a rolled piece with a plane profile and deduced the parametric equation of the die surface meshing with the noncircular billet with a plane profile [18]. According to the relative conjugate motion relationship, He et al. proposed the roll shape equation of rolling eccentric circular section shafts by the CWR process, in which the billet is rolled into a noncircular section from the wedging stage [19]. Pater et al. verified the effectiveness of the shaft with an eccentric step of a special guide rail formed by CWR through numerical simulation and experimental analyses [20, 21]. Hu et al. calculated the variation in the roll shape curve with the speed ratio and simulated the rolling process of CWR elliptical section shafts to analyse the motion characteristics and force energy parameters of the roll and rolling piece [22]. These studies provide substantial theoretical guidance for the design principle of the roll profile surface of tools and the forming mechanism of CWR for shafts with noncircular sections. However, the forming limit of noncircular section shafts in CWR has not been adequately examined in previous studies.

Accordingly, the aim of this paper is to investigate the forming principle of an elliptical section shaft formed by CWR and explore its forming limit. First, the roll's profile curve equation was deduced based on the spatial meshing relationship between the roll and rolling piece. Then, an FE model of a shaft with an elliptical section formed by CWR was established to verify the correctness of the roll's profile curve equation and analyse the forming limit. Furthermore, physical lab-scale plasticine CWR tests were carried out to validate the FE model and process feasibility. Finally, CWR was applied to form a blade preform with an elliptical section.

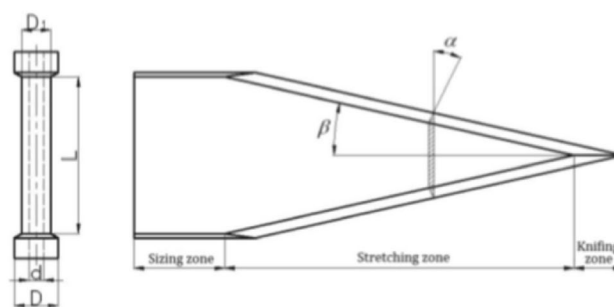


Fig. 1 Parameter sketch of the rolling piece and tool

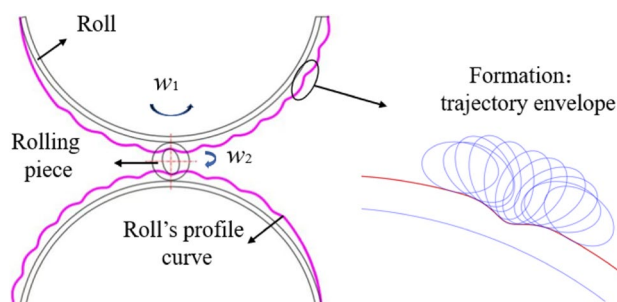


Fig. 2 Plane schematic diagram of shaft with elliptical section formed by CWR

2 Establishment of the roll profile curve equation

The forming process of a shaft with an elliptical section formed by CWR is divided into three stages: wedging, stretching and sizing, as shown in Fig. 1. The rolling piece is radially compressed and bitten by the rotating roll in the wedging stage and axially extended along the roll axis to both sides in the stretching stage. The elliptical cross-section forming accuracy is controlled by the wedge profile of the roll, and the rolling piece is finished by adjusting the number of rolling cycles in the sizing. During the whole rolling process, the rolls and the rolling piece are meshed in space and symmetrically distributed along the axial direction; hence, it is simplified to the meshing problem of the plane, as shown in Fig. 2.

As shown in Fig. 2, the CWR rolls are driven by the motor to rotate around its fixed center at an angular velocity \vec{w}_1 in the same direction, and the rolling piece is driven by the frictional force of the rolls to rotate around the fixed center of the rolls at \vec{w}_1 and at the same time around its fixed center at an angular velocity \vec{w}_2 . Therefore, the motion of the rolling piece can be analogous to the planetary motion of rotation and revolution, and the roll's profile curve can be regarded as the trajectory envelope of

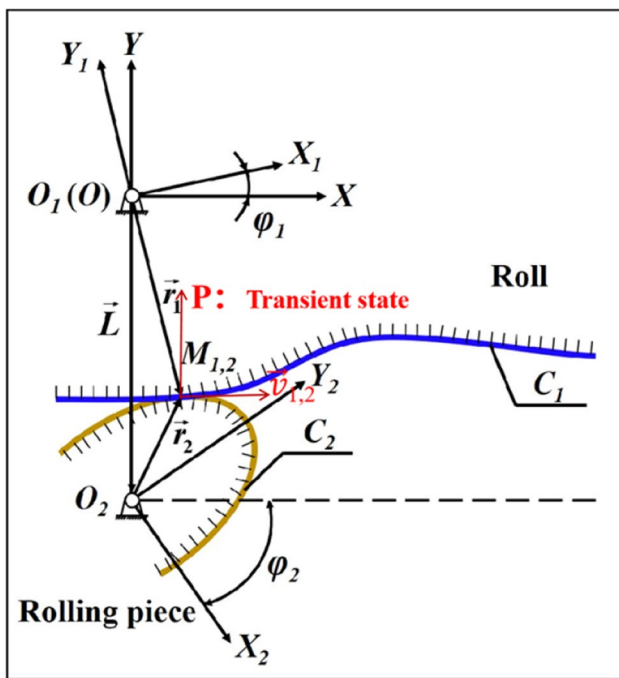


Fig. 3 Schematic diagram of the applied Cartesian coordinate systems

the rolling piece when it moves like a planet, as shown in Fig. 2.

In this section, Cartesian coordinate systems are established to construct the roll profile curve equation, as shown in Fig. 3. The coordinate systems $O_1X_1Y_1$ and $O_2X_2Y_2$ were placed at the center of the roll and the billet, respectively. Before the rolling piece rotates, axis O_1X_1 and axis O_2X_2 are parallel, as well as axis O_1Y_1 and axis O_2Y_2 . Point M is any point, represented as M_1 on the roll and M_2 on the billet, and its positions are represented by vectors \vec{r}_1 and \vec{r}_2 , respectively. Therefore, the linear velocities of M_1 and M_2 are expressed as:

$$\begin{aligned} \vec{v}_1 &= \vec{\omega}_1 \times \vec{r}_1 \\ \vec{v}_2 &= \vec{\omega}_2 \times \vec{r}_2 \end{aligned} \tag{1}$$

The vector \vec{L} is from O_2 to O_1 , and its value is the distance from the center of the rolling piece to the roll. If points M_1 and M_2 are instantaneous coincidence points, then \vec{r}_1 and \vec{r}_2 satisfy the following equation:

$$\vec{r}_2 = \vec{r}_1 + \vec{L} \tag{2}$$

The relative velocities of points M_1 and M_2 are described by Eq. (3). If points M_1 and M_2 coincide, that is, the relative velocity of point M is 0, then point M must be on the connection line between the origins of the two coordinate systems, and the point is marked with P . Then, point P is the instantaneous center of the velocity, which satisfies Eq. (4).

$$\vec{v}_{1,2} = \vec{v}_1 - \vec{v}_2 \tag{3}$$

$$\vec{v}_{1,2} \perp \vec{PM} \tag{4}$$

To ensure that the roll and the rolling piece continuously and tangentially rotate without interference and separation, then $\vec{v}_{1,2} \perp \vec{n}$, which can also be expressed as:

$$\vec{v}_{1,2} \times \vec{n} = 0 \tag{5}$$

where \vec{n} is the common normal of contact point M .

Therefore, \vec{PM} is the common normal of meshing point M . According to the meshing law, the velocity ratio at point P can be expressed by the following formula:

$$i_{1,2} = \frac{w_1}{w_2} = \frac{r_2}{r_1} = \frac{O_2P}{O_1P} \tag{6}$$

where O_1P and O_2P are the rolling radii of the rolling piece and the roll, respectively, and O_1P varies with the instantaneous radius of the rolling piece during the CWR process.

Assumingly, the coordinates of meshing point M_2 on the billet are shown in Eq. (7), and line C is the trajectory envelope formed by point M_2 in the coordinate system $O_1X_1Y_1$, which is the roll's profile curve. Through the above analysis, and according to the transformation principle of the plane coordinate system, the meshing point M_2 in the coordinate system $O_1X_1Y_1$ can be described as Eq. (8), which is the roll curve equation.

$$\vec{r}_2 = x_2(\varphi_2)\vec{i} + y_2(\varphi_2)\vec{j} \tag{7}$$

$$\begin{cases} \frac{dy_1(\theta)}{d\theta} \left[A \cos \varphi_1 - y_1(\theta) \left(1 + \frac{w_1}{w_2} \right) \right] - \frac{dx_1(\theta)}{d\theta} \left[x_1(\theta) \left(1 + \frac{w_1}{w_2} \right) - A \sin \varphi_1 \right] = 0 \\ \begin{pmatrix} x_1 \\ y_1 \\ t_1 \end{pmatrix} = \begin{pmatrix} \cos(\varphi_1 + \varphi_2) & -\sin(\varphi_1 + \varphi_2) & a \sin \varphi_2 \\ \sin(\varphi_1 + \varphi_2) & \cos(\varphi_1 + \varphi_2) & -a \cos \varphi_2 \\ 0 & 0 & 1 \end{pmatrix} \begin{pmatrix} x_2 \\ y_2 \\ t_2 \end{pmatrix} \end{cases} \tag{8}$$

where φ_1 and φ_2 are arbitrary angles during rolling; x_1 and y_1 are the positions of point M_1 in the coordinate system $O_1X_1Y_1$ of the roll; x_2 and y_2 are the positions of point M_2 in the coordinate system $O_2X_2Y_2$ of the billet; and t_1 and t_2 are the supplementary coordinates of meshing point M_1 (M_2) along the axial direction.

3 Research arrangements

3.1 Finite element simulation

To verify the correctness of the roll's profile curve equation and explore the forming limit of the shaft with an elliptical

section formed by CWR, the corresponding FE model was established in this section.

An example is shown as follows: the contour parameter equation of the shaft with an elliptical section is shown in Eq. (9). Due to the profile symmetry of the elliptical section, half of the section profile is used to derive the roll’s profile curve equation. At the same time, the forming process corresponding to half of the section profile is defined as one rolling cycle. Compared with the whole rolling process, the rolling time corresponding to one rolling cycle is very short, thereby ignoring the change in the speed ratio in one rolling cycle. However, it is difficult to accurately measure the velocity ratio as the rolling radius r_1 is constantly changing, so the parameter of the rolling radius of billet r_b is introduced, and the quantitative relationship between the rolling radius of billet r_b and the velocity ratio is shown in Eq. (10).

Combined with Eqs. (7–9), the profile curve equation of the CWR shaft with an elliptical section is obtained as Eq. (11).

$$\begin{cases} x_2 = a \cos \theta \\ y_2 = b \sin \theta \end{cases} \quad (9)$$

$$r_b = \frac{L}{1 + w_1/w_2} = \frac{L}{1 + i_{1,2}} \quad (10)$$

$$\begin{cases} x_1 = a \cos \theta \cos\left(\frac{L\varphi_1}{a-r_b}\right) - b \times \sin \theta \sin\left(\frac{L\varphi_1}{a-r_b}\right) + A \sin\left(\frac{r_b\varphi_1}{L-r_k}\right) \\ y_1 = a \cos \theta \sin\left(\frac{L\varphi_1}{L-r_b}\right) + b \sin \theta \cos\left(\frac{L\varphi_1}{L-r_b}\right) - A \cos\left(\frac{r_b\varphi_1}{L-r_b}\right) \theta \in (-\pi/2, \pi/2) \\ \varphi_1 = \arccos\left(\frac{(b^2-a^2)\cos\theta\sin\theta}{r_k \sqrt{(b\cos\theta)^2 + (a\sin\theta)^2}}\right) - \arctan\left(\frac{a}{b} \tan\theta\right) \end{cases} \quad (11)$$

where a and b represent the major and minor axes of the ellipse, respectively, and their values are 18 and 14, respectively, in the example. The initial radius r_0 of the billet is selected as 20 mm. Based on the existing studies [22], the rolling cycles were determined to be 8. As seen from Eqs. (10) and (11), the rolling radius of billet r_b is a key parameter for solving the roll’s profile curve equation, which remains

unchanged in one rolling cycle but changes regularly during the entire rolling process. The distribution of r_b in each rolling cycle is shown in Fig. 4a via multiple optimizations. The roll’s profile curve equation was solved via MATLAB, and the corresponding curve is represented in Fig. 4b. Evidently, r_b in the wedging stage is slightly larger than r_0 and gradually decreases to close to r_0 as the deformation continues. The r_b in the stretching and sizing stages continues to decrease to lower than r_0 , showing a variation trend consistent with the literature [22]. In addition, the forming and stretching angles α and β of the roll were selected to be 28° and 10° , respectively.

The process of the CWR elliptical section shaft was simulated via the FE software DEFORM-3D. Half of the geometric model was adopted to improve the calculation efficiency, as shown in Fig. 5. The roll and guide plate were set to be rigid bodies owing to their small and negligible plastic deformation, and the rolling piece was set to be a plastic body because its elastic deformation can be ignored. The shear friction model was applied, and the friction coefficients between the billet and two rolls and the billet and two guide plates were 0.9 and 0.3, respectively. The material of the billet was TC6 titanium alloy, and the material properties of TC6 titanium alloy, has been discussed in reference

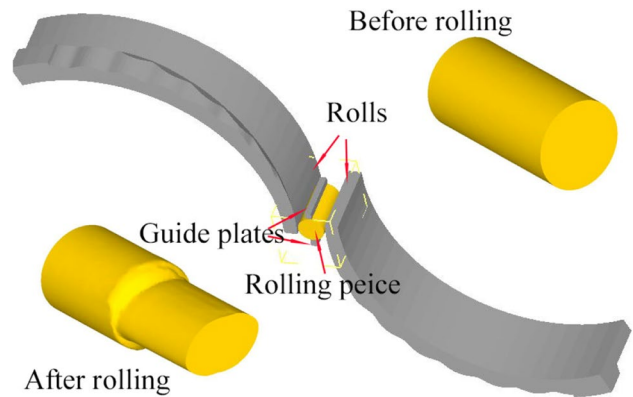
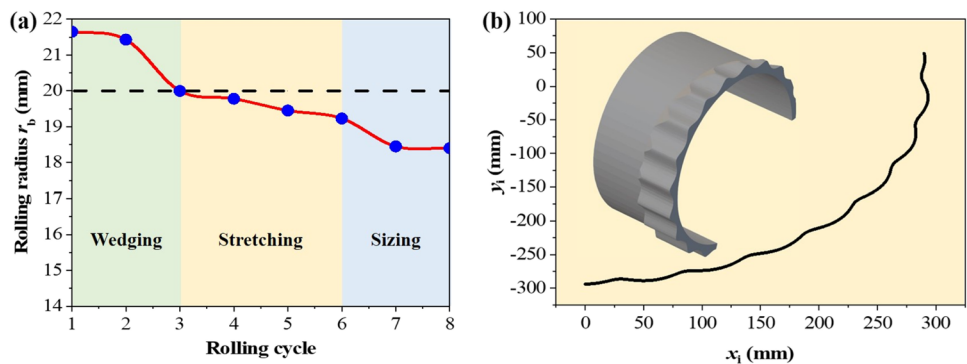


Fig. 5 The FE model of the CWR elliptical section shaft

Fig. 4 a The variation in the rolling radius in the different rolling cycles and b the calculated profile curve



[22]. The initial deformation temperature was determined to be 960 °C, the convection coefficient between the ambient air and billet was $20 \text{ W}\cdot\text{m}^{-1}\cdot\text{K}^{-1}$, and the thermal contact conductance between the rolls and billet was $10 \text{ kW}\cdot\text{m}^{-2}\cdot\text{K}^{-1}$ [23, 24].

3.2 Cross wedge rolling experiments

Zhou et al. demonstrated that CWR soft model materials, such as plasticine, can well reflect the forming characteristics of CWR metal materials under the same process conditions, which effectively shortens the research cost and cycle [25]. Therefore, a physical lab-scale platform for CWR plasticine was designed to validate the reliability of the established FE model, as shown in Fig. 6. It was mainly composed of a base frame, an electric source, a drive, a step motor, a pair of flat dies, and a controller. The forming

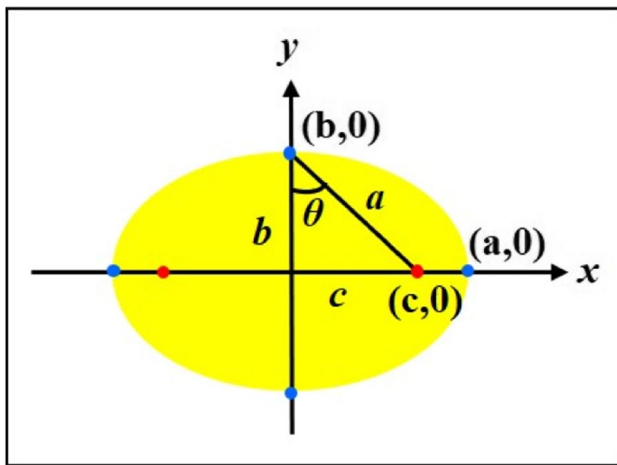
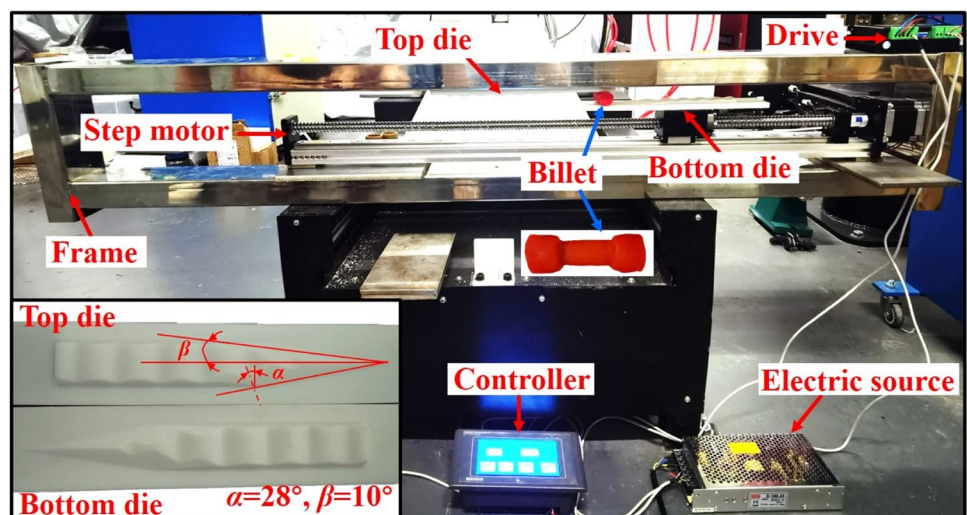


Fig. 6 Illustrations of the CWR experimental platform and forming wedge tools

Fig. 7 The forming process of the CWR elliptical section shaft















wedge tools were 3D printed by a Fortus 400mc using acrylonitrile butadiene styrene. During the CWR process, the top die was fixed on the base frame with hot melt adhesive, and the bottom die was driven by the step motor at a velocity of 80 mm/s. The rolling piece material was German weiblenet plasticine, which needs to be kept in a thermostat at 11 °C for 2 h before deformation. CWR experiments were performed three times to guarantee the accuracy of the results under the same deformation conditions.

3.3 Feasibility verification of the CWR elliptical shaft

The elliptical section shaft with an eccentricity e of 0.75 was rolled and simulated via the designed dies based on the established roll's profile curve equation, and the eccentricity e will be discussed in Sect. 4. Figure 7 represents the forming process of the shaft with an elliptical section during CWR. The rolling piece was wedged from the symmetry plane. The metal of the rolling piece was compressed radially and extended axially to both sides simultaneously. Under the force of the roll's profile surface, the elliptical profile of the rolling piece was gradually rolled into shape at the beginning of the wedging stage according to the spatial meshing motion and finally formed into an elliptical section after the sizing stage. Notably, the inner inclined step is irregularly spiral since there is no transition wedge between the widening and sizing stages.

The experimental and simulated rolled pieces were measured and compared to quantitatively evaluate the accuracy of the established FE model, as shown in Fig. 8a. The errors in the $2a$ (i.e., maximum diameter) and $2b$ (i.e., minimum diameter) are less than 0.60 mm and 0.68 mm, demonstrating that the established FE model can well reflect the geometric dimensions of the elliptical section shaft in CWR. In addition, compared with the target

Fig. 8 **a** Comparison of the FE simulation and CWR experiment and **b** longitudinal sections of the plasticine rolled piece

Eccentricity e	Quality in the axial direction	Quality of cross section profile
0	No spiral 	continuous and smooth 
0.25	Slight spiral 	continuous and smooth 
0.5	Slight spiral 	continuous and smooth 
0.75	Slight spiral 	continuous but slightly matte 
0.8	Sever spiral and slight matte 	continuous but sever matte 
0.85	Sever necked 	
0.9 and 0.95	Sever necked even pulled off 	

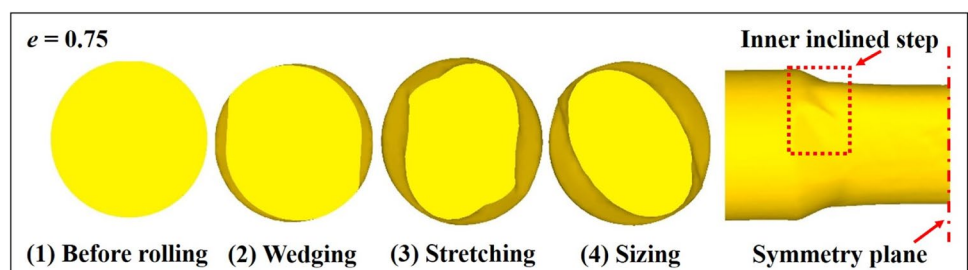
dimensions calculated theoretically, the error of 2a and 2b of the experimental rolled pieces is less than 1.35 mm, indicating that elliptical section shafts with good forming quality can be manufactured via the designed dies based on the established roll profile curve equation. Furthermore, the experimental rolled pieces were cut longitudinally to observe their internal forming quality, as shown in Fig. 8b. Evidently, there are no internal defects inside the rolled piece, but further research is needed on the internal defects of the elliptical shaft of CWR metal materials.

4 Forming limit analysis and application

4.1 Forming limit analysis

The forming limit of the elliptical section shaft in CWR is to form an elliptical section that is as flat as possible under the premise of ensuring continuous and stable rotation, thereby reducing the deformation amount of subsequent forging. Therefore, the eccentricity e was used to represent the flatness of the elliptical section, which is also a significant indicator when determining the forming limit of elliptical section shafts, as shown in Fig. 9 and given in

Fig. 9 Schematic of the eccentricity of the elliptical section



Eq. (12). Mathematically, the value range of e is $0 < e < 1$ when the eccentricity e of the circular section is 0. The larger the eccentricity e is, the flatter the elliptical section. The forming limits of CWR were discussed via the FE model by numerical simulation with e values of 0, 0.25, 0.5, 0.75, 0.8, 0.85, 0.9, and 0.95.

$$e = \sin\theta = c/a = \sqrt{a^2 - b^2}/a \tag{12}$$

The quality evaluation index of the rolling pieces with different e consists of two parts, namely, whether there is a spiral in the axial direction and whether the cross-section profile is continuous and smooth, and the results are listed in Fig. 10. When the eccentricity e is 0.85, 0.9, and 0.95, the billets are severely necked or even pulled off and cannot be successfully formed. This is related to the excessive deformation of the rolling piece, as shown in Fig. 11. For the shaft with an elliptical section, two area reductions can be

theoretically calculated according to the deformation of the major and minor axes, and the maximum area φ_{max} is used to characterize the defoamiton. There is a positive correlation between the eccentricity e and area reduction φ_{max} , and the area reduction φ_{max} is as high as 80% when the eccentricity e is 0.8, which is very detrimental to the stable rotation and easily causes severe necking or even pull off of the rolling piece.

However, when the eccentricity e is less than 0.8, the rolling piece can be normally formed, but the forming quality is different. When the eccentricity e is less than 0.5, there is no obvious spiral in the axial direction of the rolling piece, and the cross-section profile is also continuously smooth. When the eccentricity e continues to increase, the spiral in the axial direction of the billet becomes more obvious, and the smoothness of the cross-sectional profile decreases. Therefore, the conclusion can be inferred that eccentricity e should be less than 0.8 when using cross-wedge rolling to form a shaft with an elliptical section. In other words, the forming limit of the elliptical section shaft in cross wedge rolling is approximately 0.8.

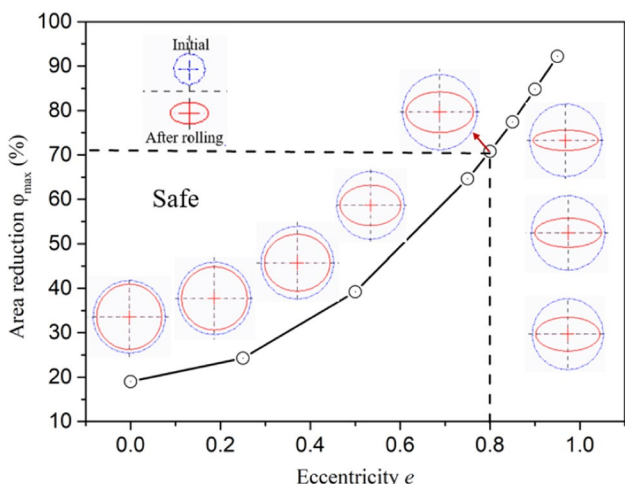
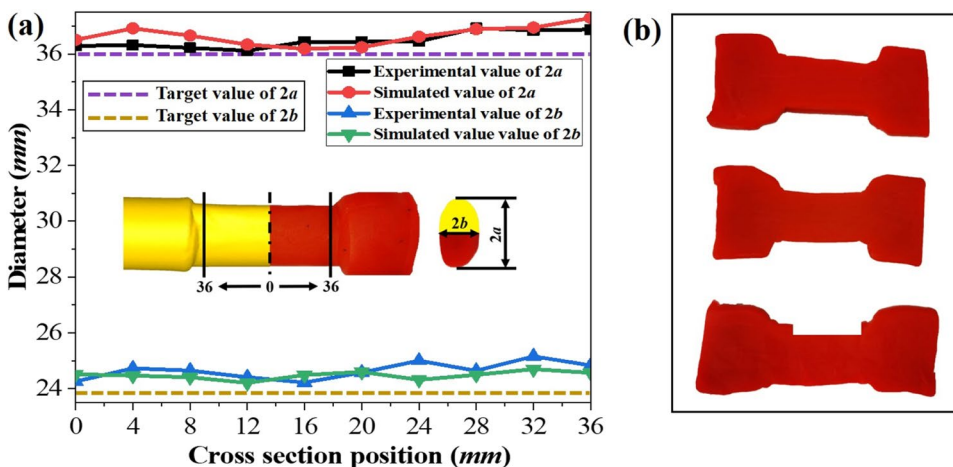


Fig. 10 Forming quality of cross wedge rolling for elliptical section shafts with different eccentricities

4.2 Application

Figure 12 shows a titanium alloy blade with a complex shape for an aero-engine compressor. The blade with a single tenon is thin and twisted at a certain angle, the damping table is located in the middle of the blade body, and the volumes of the blade tip part and the tenon are very different. Based on the equal area criterion, a variable diameter preform with a circular cross-section was prepared by the CWR process, and detailed information has been published in the literature [16]. However, since the shape of the blade body is flat, it will be more beneficial to reduce the difficulty of isothermal forging as well as improve the material utilization if a preform with an elliptical section can be manufactured.

Fig. 11 The relationship between the eccentricity and area reduction



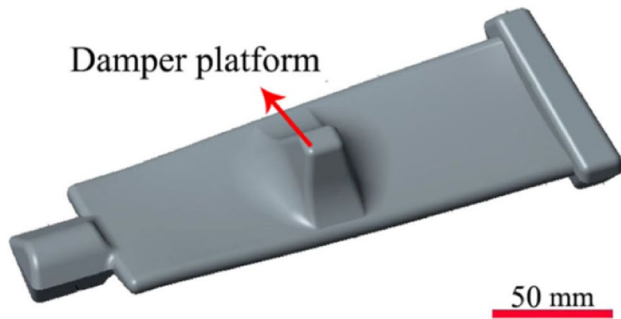


Fig. 12 Titanium alloy blade for an aero-engine compressor

Therefore, a preform with an elliptical section was designed on the basis of previous research.

According to the calculated diameter based on the equal area criterion, as shown in Fig. 3 in the literature [16], the preforms are optimized as elliptical sections except for the damper platform and tenon, as shown in Fig. 13c. The eccentricity e and short axis are set to be 0.75 and 22 mm, respectively, to ensure the forming equality and flatness of the preform as much as possible. Meanwhile, since the preform is asymmetrical in the axial direction, it can be rolled in pairs, which can make the force on both sides of the workpiece symmetrical and double the production efficiency. The roll is designed with two wedges according to the shape characteristics of the preform. The first wedging, widening and finishing is to form the blade tip of the damper platform, and the second is to form the damper platform to the tenon. In addition, the forming angle and stretch angle are selected as 25° and 7.5° based on previous research [16, 17]. Therefore, the rolls for the blade preform with an elliptical section formed by CWR are shown in Fig. 14.

Figure 15 a shows the CWR rolling process of a preform with an elliptical section. It can be seen that the preform with the elliptical section has good surface quality, the elliptical sections are continuously smooth, and there is no spiral in the widening section. However, one thing is very striking that there are spirals on the right side of the

Fig. 13 The equivalent radii distribution of preforms with circular and elliptical sections

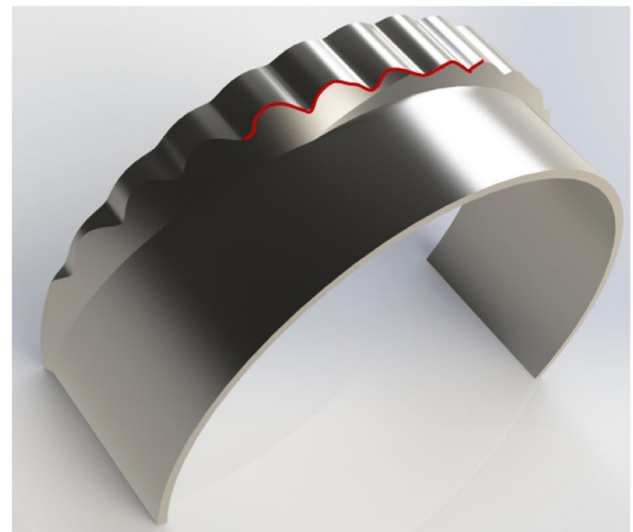
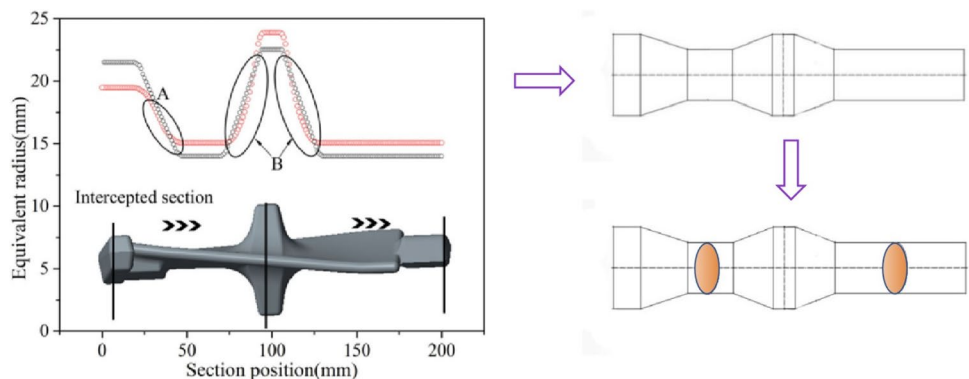


Fig. 14 The roll for the blade preform with an elliptical section formed by CWR

damper platform that can be seen as an inner step, and it is also the place where the elliptical section gradually transitions to the circular section. Therefore, when designing the roll profile curve at this position, on the basis of considering the reserved rolling curve, the deformation caused by the excessive section shape should also be considered. Another issue that needs to be clarified is that if there are more than two elliptical sections in the rolling piece, it is best to ensure that the major and minor axes are in the same direction to avoid interference. In the rolling blade preform, we try to make the major and minor axes of the two elliptical sections in the same direction by adjusting the rolling cycle or the roll profile curve. If simply adjusting the rolling cycle cannot meet the requirements, it may be necessary to adjust the eccentricity e and initial diameter of the rolling piece, and further research is needed and in progress.

Figure 16 represents the blade manufactured by isothermal forging of the preform with elliptical section by numerical simulation. It can be found that the edge of the

Fig. 15 The CWR rolling process of a preform with an elliptical section: **a** rolling process; **b** forming quality of the cross section

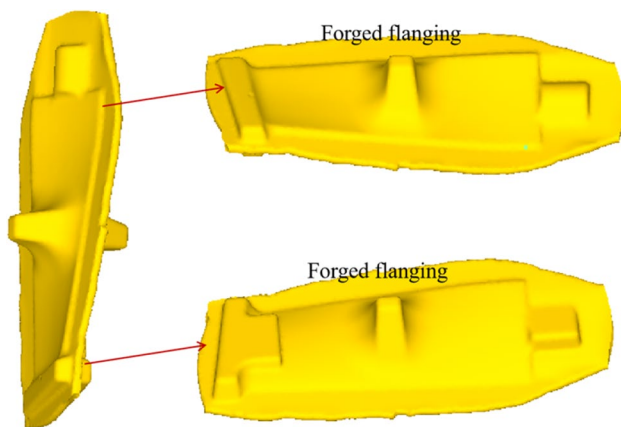
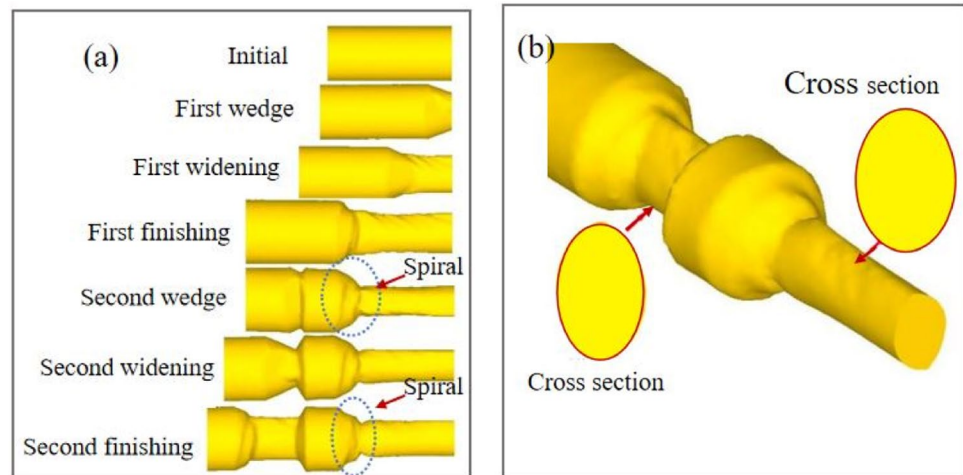


Fig. 16 The isothermal forging blade manufactured by the preform with elliptical section

forged blade is continuous and smooth, and without obvious defects such as folding and fracture. However, there are still relatively abundant forging forged flanging, which can be adjusted by further optimizing the volume distribution.

In summary, it is feasible to use CWR to manufacture blade preforms with two elliptical sections, and the research results can also be extended and applied to the preforms of nonrotating parts, such as connecting rods, as well as provide guidance for shafts with elliptical sections of other materials formed by CWR, such as carbon steel and nickel-based alloys.

5 Conclusions

1. According to the plane meshing principle between the roll and the rolling piece, the roll's profile curve equation is deduced and well verified by FE analysis and CWR experiments with plasticine through a self-built

platform, and the error of the experimental rolled pieces is less than 1.35 mm compared with the target dimensions, indicating that good forming quality can be manufactured via the designed roll's profile curve equation.

2. The accuracy of the established FE model was tested by quantitatively evaluating the diameters of the experimental and simulated rolled pieces, and the errors maximum and minimum diameters are less than 0.60 mm and 0.68 mm, respectively, which can well reflect the geometric dimensions of the elliptical section shaft in CWR.
3. Eccentricity e is used to assess the flattening of the shaft with an elliptical section, and the forming limit is approximately 0.8 (i.e., $e \leq 0.8$) by numerical simulation analysis.
4. A blade preform for an aero-engine compressor was designed with two elliptical sections, and it was well formed by the FE model, which verified the feasibility. The research results can also be extended and applied to the preform of other nonrotating parts and other materials. However, many problems, such as the rolling curve of the inner steps and the major and minor axes in the same direction, require further research.

Author contribution Junling Li: software, investigation, validation, methodology, writing—original draft. Weicheng Chu: software, methodology. Pengni Feng: validation, writing—review and editing. Baoyu Wang: project administration, supervision. Ping Chen: supervision, writing—review and editing. Shuang Fang: investigation, writing—review and editing.

Funding The research was funded by the National Natural Science Foundation of China (Grant No. 52205329). This work is also supported by the Beijing Key Laboratory of Metal Forming Lightweight.

Declarations

Competing interests The authors declare no competing interests.

References

- Liu YL, Yang H, Zhan M, Fu ZX (2002) A study of the influence of the friction conditions on the forging process of a blade with a tenon. *J Mater Process Technol* 123:42–46
- Na YS, Yeom JT, Park NK, Lee JY (2003) Prediction of microstructure evolution during high temperature blade forging of a Ni–Fe based superalloy, alloy 718. *Metal Mater Int* 9:15–19
- Huang SH, Zong YY, Shan DB (2013) Application of thermo-hydrogen processing to Ti6Al4V alloy blade isothermal forging. *Mater Sci Eng, A* 561:17–25
- Painter B, Shivpuri R, Altan T (1996) Prediction of die wear during hot-extrusion of engine valves. *J Mater Process Technol* 59:132–143
- Pater Z, Bartnicki J, Samotyka G (2005) Numerical modelling of cross-wedge rolling process of ball pin. *J Mater Process Technol* 164–165:1235–1240
- Huo YM, Bai Q, Wang BY, Lin JG, Zhou J (2015) A new application of unified constitutive equations for cross wedge rolling of a high-speed railway axle steel. *J Mater Process Technol* 223:274–283
- Yang CP, Dong HB, Hu ZH (2018) Micro-mechanism of central damage formation during cross wedge rolling. *J Mater Process Technol* 252:322–332
- Li Q, Lovell MR, Slaughter W, Tagavi K (2002) Investigation of the morphology of internal defects in cross wedge rolling. *J Mater Process Technol* 125:248–257
- Pater Z, Gontarz A, Weroński W (2006) Cross-wedge rolling by means of one flat wedge and two shaped rolls. *J Mater Process Technol* 177:550–554
- Pater Z (2010) Development of cross-wedge rolling theory and technology. *Steel Res International* 81:25–32
- Ji HC, Liu JP, Wang BY, Zhang ZR, Zhang T, Hu ZH (2015) Numerical analysis and experiment on cross wedge rolling and forging for engine valves. *J Mater Process Technol* 221:233–242
- Ji HC, Liu JP, Wang BY, Fu XB, Xiao WC, Hu ZH (2017) A new method for manufacturing hollow valves via cross wedge rolling and forging: Numerical analysis and experiment validation. *J Mater Process Technol* 240:1–11
- Shen JX, Wang BY, Zhou J, Lin LF, Liu SQ, Feng PN (2020) Investigation on the inner hole spiral-groove of cross wedge rolling of hollow shafts with mandrel. *Int J Adv Manuf Technol* 110(7–8):1773–1787
- Shen JX, Wang BY, Yang CP, Zhou J, Cao XQ (2021) Theoretical study and prediction of the inner hole reduction and critical mandrel diameter in cross wedge rolling of hollow shaft. *J Mater Process Technol* 294:117140
- Gan HY, Cheng M, Song HW, Chen Y, Zhang SH, Vladimir P (2019) Microstructure evolution and dynamic recrystallization mechanism of GH4169 alloy during cross wedge rolling. *Rare Metal Mater Eng* 11(48):3556–3562
- Li JL, Wang BY, Fang S, Chen P (2020) Investigation of the microstructure evolution and mechanical properties of a TC6 alloy blade preform produced by cross wedge rolling. *Archiv Civ Mech Eng* 20:70
- Liang JC, Bai ZB, Li DP, Ren GS (1996) Research on shaped surface of cross wedge rolling of non-rotary shaft. *Trans Chin Soc Agric Mach* 2:154–160
- He T, Wang BY, Hu ZH (2008) Numerical simulation on cross wedge rolling of shaft parts with eccentric section. *Forging Stamping Technol* 1(33):53–55
- Pater Z, Gontarz A, Weroni W (2008) Cross rolling of parts with non-circular cross section. *Archiv Civ Mech Eng* 8(2):139–147
- Pater Z (2011) Cross-wedge rolling of shafts with an eccentric step. *Int J Iron Steel Res* 18(6):26–30
- Hu FG, Wang BY, Hu ZH (2009) Study on key technologies of shaft parts with elliptical section formed by cross wedge rolling. *Forging Stamping Technol* 5(34):71–74
- Li JL, Wang BY, Huang H, Fang S, Chen P, Shen JX (2018) Unified modelling of the flow behaviour and softening mechanism of a TC6 titanium alloy during hot deformation. *J Alloy Compd* 748:1031–1043
- Li JL, Wang BY, Fang S, Chen P (2019) Investigating the effects of process parameters on the cross wedge rolling of TC6 alloy based on temperature and strain rate sensitivities. *Int J Adv Manuf Technol* 103:2563–2577
- Pater Z (2006) Finite element analysis of cross wedge rolling. *J Mater Process Technol* 173:201–208
- Zhou XY, Shao ZT, Zhang C, Sun FZ, Zhou WB, Hua L, Jing J, Wang LL (2020) The study of central cracking mechanism and criterion in cross wedge rolling. *Int J Mach Tools Manuf* 159:103647

Publisher's note Springer Nature remains neutral with regard to jurisdictional claims in published maps and institutional affiliations.

Springer Nature or its licensor (e.g. a society or other partner) holds exclusive rights to this article under a publishing agreement with the author(s) or other rightsholder(s); author self-archiving of the accepted manuscript version of this article is solely governed by the terms of such publishing agreement and applicable law.